J. Geophys. 44, 341–352, 1978

Journal of Geophysics

Measurements of Anisotropy of Magnetic Susceptibility Using Inductive Magnetometers *

H. Scriba and F. Heller

Institut für Geophysik, ETH Zürich, CH-8093 Zürich, Switzerland

Abstract. At present the instruments most commonly used for sensitive measurement of remanent and induced magnetization of rocks are spinner magnetometers and cryogenic magnetometers. The analysis of magnetic susceptibility anisotropy with these instruments is described in this paper with special emphasis on measurements with the cryogenic magnetometer. Problems arising from finite specimen size are discussed. It is shown that the optimum length-to-diameter ratio for a cylindrical specimen is 0.90 ± 0.02 for the spinner magnetometer used and 0.86 ± 0.02 for the cryogenic magnetometer. Comparative measurements of magnetic anisotropy obtained from the two instruments yield good agreement. In order to demonstrate the performance of the cryogenic magnetometer in measuring magnetic susceptibility anisotropy, a regional investigation has been carried out. The main plane of anisotropy is observed to be consistent with the macroscopic rock fabric.

Key words: Magnetic susceptibility anisotropy – Cryogenic magnetometer – Spinner magnetometer.

1. Introduction

Rock magnetism has become a very important branch of geophysics during the last two decades. This is mainly due to the observation that rocks containing ferromagnetic minerals are able to conserve the magnitude and direction of the magnetic field in which they cooled down or were deposited. This is the basis for studying the history of the Earth's magnetic field and associated phenomena such as continental drift and polar wandering.

One of the principal assumptions of palaeomagnetism is that the direction of magnetization is parallel to the magnetizing field. This is only true as long as the material is magnetically isotropic, i.e. the magnetic susceptibility is a scalar. However, many rocks are anisotropic and the susceptibility must be represented

* Contribution No. 199, Institut für Geophysik, ETH Zürich

0340-062X/78/0044/0341/$02.40

by a symmetrical tensor of second order. The corresponding geometrical body is an ellipsoid. Thus, for palaeomagnetic investigations of strongly anisotropic rocks, the direction of magnetization has to be corrected for anisotropy. Moreover, the observed anisotropy is closely related to rock fabric and can be used as a tool in structural analysis of rocks.

Magnetic anisotropy was first observed in sediments by Ising (1943). It has been shown that this anisotropy is mostly caused by mechanical forces acting during deposition (e.g. Granar, 1958; Rees, 1961), the minimum axis of susceptibility being aligned perpendicular to the bedding plane. The structure of igneous rocks can also be determined by anisotropy measurements (cf. e.g. Heller, 1973). In these rocks the macroscopic schistosity planes usually coincide with the main anisotropy plane which is defined as the plane containing the maximum and intermediate principal axes of anisotropy. A comprehensive review on magnetic anisotropy is given by Bhathal (1971).

In principle the anisotropy of magnetic susceptibility can be observed using any instrument which measures the bulk susceptibility in a certain direction, e.g. the transformer bridge (cf. Fuller, 1960; Kubli, 1967). Of course, anisotropy can also be studied with instruments measuring only the difference between the maximum and minimum susceptibility (in the plane of measurement) and its phase, e.g. the torque meter (Stone, 1967; Scriba, 1967) or the spinner magnetometer (cf. Kent and Lowrie, 1975). Most early investigations were carried out using the torque meter. In this instrument the rock sample is suspended from a thin wire. When a horizontal field is applied, the specimen is deflected by a small angle due to its remanence and anisotropy of susceptibility. The effect of remanence, of course, can be avoided by using AC fields. Either low fields (cf. Granar, 1958; King and Rees, 1962; Scriba, 1967) or high fields have been used (cf. Stacey, 1960). The other instrument commonly used now is the spinner magnetometer (cf. Noltimier, 1967; Berset, 1968; Heller, 1973). This paper adds the cryogenic magnetometer to the instruments measuring magnetic susceptibility anisotropy.

2. Method of Measurement

The measurements were carried out using a Digico spinner magnetometer with anisotropy head and a ScT cryogenic magnetometer. These instruments are called inductive magnetometers in this paper because the signal induced by the field of a magnetized rock sample is analysed.

2.1. Spinner Magnetometer

Only a brief outline of the method of measurement will be given here. In principle the method is identical to that when measuring remanent magnetization with the only difference that a magnetic field is applied which causes an induced magnetization in the specimen. If the rotating specimen has a susceptibility difference in the plane of measurement, it produces a signal in the sensor coils the frequency of which is twice the frequency of rotation; the amplitude and phase of the anisotropy signal depend upon the susceptibility tensor elements in the measurement plane. Measurements in three perpendicular planes of a specimen provide the complete susceptibility matrix. Its eigenvalues and eigenvectors can be found by transforming to principal axes.

The Digico anisotropy meter uses two orthogonally arranged coils one of which is excited at an audio frequency. A signal is only detected in the sensor coil, if the sample is anisotropic in the plane of measurement (cf. Eq. (8b)). The corresponding elements of the susceptibility matrix are computed on line by harmonic analysis. The coils of our Digico anisotropy meter are very close to the sample. There is a new version on the market now which has a slightly larger detector distance.

2.2. Cryogenic Magnetometer

Essentially this instrument is a modern version of the ballistic magnetometer. The instrument we have in use consists of three pairs of Helmholtz pickup coils which are kept in a superconducting state. If a magnetized sample is inserted into the coils a persistent current is initiated in each coil pair which is proportional to the component of magnetization of the sample along the corresponding coil axis (for details see Goree and Fuller, 1976).

Besides of remanence measurements the cryogenic magnetometer can also be used for measuring bulk susceptibility and its anisotropy. The method is very simple. A field of a few Oersteds – we have used $H = 1.01$ Oe – is applied to the sensor coils. After cooling below the critical temperature for superconductivity, this field is permanently retained in the system. A sample inserted into the coils will now produce a signal S which is the sum of the induced (I_i) and the remanent component (R_i) of magnetization multiplied by the volume (V) of the specimen

$$S_i = (R_i + I_i) \cdot V \tag{1}$$

with $i = \xi, \eta, \zeta$ (coordinate system of the specimen). This can also be written in vector form

$$\mathbf{S} = (\mathbf{R} + \mathbf{I}) \cdot V \tag{2}$$

where the induced magnetization is proportional to the applied field H

$$\mathbf{I} = K \cdot \mathbf{H} \tag{3}$$

with K = magnetic susceptibility tensor. This tensor is symmetrical and of second order

$$K = \begin{pmatrix} k_{\xi\xi} & k_{\xi\eta} & k_{\xi\zeta} \\ k_{\eta\xi} & k_{\eta\eta} & k_{\eta\zeta} \\ k_{\zeta\xi} & k_{\zeta\eta} & k_{\zeta\zeta} \end{pmatrix} . \tag{4}$$

In our measuring procedure a field is applied parallel to the x-axis of the instrument with the ζ-axis of the specimen coinciding with the z-axis of the

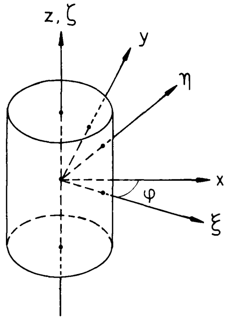

Fig. 1. Orientation of the specimen with the coordinates ξ, η, ζ with respect to the instrument's coordinates x, y, z

instrument. The specimen will now be rotated around this axis such that ξ and η lie in the plane of measurement (Fig. 1). For any position the components of the magnetic field H in coordinates of the specimen are given by

$$H_\xi = H \cdot \cos\varphi \qquad \text{and } H_\eta = H \cdot \sin\varphi. \tag{5}$$

Inserting into (3) we obtain for the components of the induced magnetization

$$\begin{aligned} I_\xi &= H(k_{\xi\xi}\cos\varphi + k_{\xi\eta}\sin\varphi) \\ I_\eta &= H(k_{\xi\eta}\cos\varphi + k_{\eta\eta}\sin\varphi). \end{aligned} \tag{6}$$

The corresponding expressions in the coordinate system of the instrument are

$$\begin{aligned} I_x &= I_\xi \cos\varphi + I_\eta \sin\varphi \\ I_y &= -I_\xi \sin\varphi + I_\eta \cos\varphi. \end{aligned} \tag{7}$$

Inserting (6) into (7) yields

$$I_x = H[\tfrac{1}{2}(k_{\xi\xi} + k_{\eta\eta}) + \tfrac{1}{2}(k_{\xi\xi} - k_{\eta\eta})\cos 2\varphi + k_{\xi\eta}\sin 2\varphi] \tag{8a}$$

$$I_y = H[\tfrac{1}{2}(k_{\eta\eta} - k_{\xi\xi})\sin 2\varphi + k_{\xi\eta}\cos 2\varphi]. \tag{8b}$$

We now turn the specimen such that ξ and η, respectively, are parallel to z. The corresponding expressions are easily derived from (8) by cyclic exchange.

As can be seen from (8) it would be sufficient to make two measurements at an angle $\varphi = 0°$ and $\varphi = 90°$ in order to determine the k_{ik}. In practice, however, the specimen has a remanent magnetization which has to be eliminated. Moreover, there is instrumental drift. The first problem can be solved by repeating the measurements at 180° and 270°, taking advantage of the different periodicities of the remanent magnetization R and the induced magnetization I, i.e. 2π and π, respectively. Thus by taking the arithmetic mean of two readings with a phase shift of π, the influence of remanence is cancelled. On the other hand the remanence can be determined by taking the difference of the readings. Actually we have taken readings in steps of 45° from 0° to 360° in order to improve the quality of data which are later used for the computation of the anisotropy ellipsoid. Instrumental drift is taken into account by comparing the readings at

0° and 360° and correcting the values measured in between by linear interpolation of the difference. Instrumental drift is of the order of $1 \cdot 10^{-8}\,G$ equivalent magnetization during the measurements in one plane which take about 40 s. This value is well below the errors introduced by instability of remanence which are of the order of $1 \cdot 10^{-7}\,G$ for the specimens measured.

The measurements are repeated for the $\eta\zeta$- and the $\zeta\xi$-plane, respectively. Then the susceptibility ellipsoid can be computed by a transformation to the principal axes (Granar, 1958; Scriba, 1967).

As the susceptibility matrix K is real and symmetrical, the transformation to principal axes can easily be carried out using the Jacobi method (cf. e.g. Sperner, 1961). A FORTRAN program for this computation can be obtained from the authors upon request. The program uses the data from the cryogenic magnetometer as input. Remanent magnetization and instrumental drift have already been eliminated according to the procedure described previously. The program can also be used for any other kind of anisotropy measurements by simply adapting the input. It also serves as the fundamental program for the Digico anisotropy meter.

3. Effects of Specimen Shape and Size

For practical convenience cylindrical rock specimens are used for magnetic investigations. Ideally a specimen should have spherical shape. Then, even for finite distances between sample and sensor, it would act like a dipole at its centre provided that the magnetization is uniform. However, as we are working with cylindrical specimens, even for isotropic rocks an apparent anisotropy results which is caused by the shape of the specimen and the finite distance to the sensor.

3.1. Effect of Specimen Shape

This effect is caused by the different demagnetization factors along the axes of the specimen. It is given by Rees (1965)

$$\frac{\Delta k}{k} = k \cdot \frac{N_z - N_r}{(1 + N_z k)(1 + N_r k)} \tag{9}$$

where N_z is the demagnetizing factor along the axis of the cylinder and N_r is the demagnetizing factor in the radial plane. Shape induced anisotropy will be zero if $N_z = N_r$. The demagnetizing factors for cylinders with different ratios of length to diameter have been computed by Sharma (1966). N_z and N_r have been plotted against the ratio of length to diameter in Figure 2. They are equal for $l/d = 0.9185$. However, as can be seen from Equation (9) and Figure 2 the influence of an error of 10% in the length to diameter ratio will be negligible $\left(\frac{\Delta k}{k} < 10^{-3}\right)$

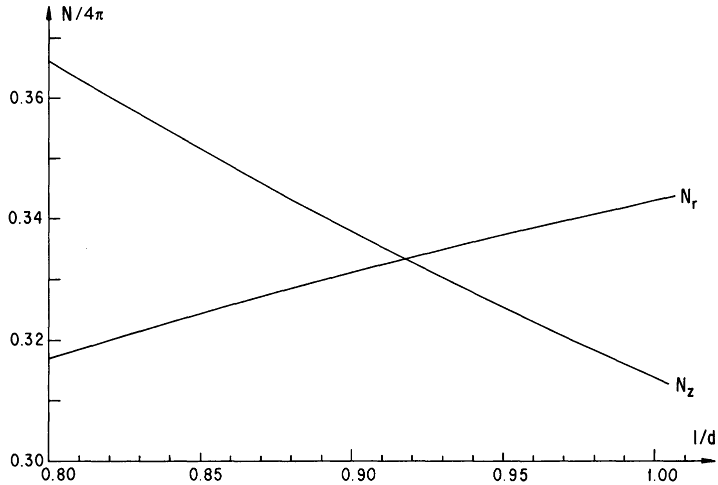

Fig. 2. Axial (N_z) and radial (N_r) demagnetizing factors as a function of length-to-diameter ratio l/d for cylindrical specimens

if the bulk susceptibility does not exceed 10^{-3} G/Oe (see also Kent and Lowrie, 1975). Higher bulk susceptibilities are very unusual in rocks (Sharma, 1976) and therefore the specimen *shape* effect can generally be neglected.

3.2. *Effect of Specimen Size*

The other effect that may cause errors in anisotropy measurements comes from the finite specimen size. It applies only when using inductive magnetometers such as spinner magnetometers where the field produced by a rotating sample is measured by a sensor at a finite distance from the sample. However, when using other instruments, e.g. a torque meter where the torsion caused by the interaction of the applied field with the magnetized sample is measured, the specimen size is unimportant. Of course, this is only true if the field is homogeneous in the region of the sample.

In order to obtain a high sensitivity with inductive magnetometers a relatively small specimen-sensor distance is required. Therefore the specimen no longer can be treated as an infinitesimal dipole. The corresponding formulae have been derived by Sharma (1964) and a brief summary will be given here. Only two planes of measurement need to be considered because of the axial symmetry of a cylindric specimen. The axial field of a uniformly magnetized cylinder of length l, radius r at a distance a from its centre is given by

$$H_z = 2\pi \cdot I_z \left[\frac{a + l/2}{\sqrt{r^2 + (a + l/2)^2}} - \frac{a - l/2}{\sqrt{r^2 + (a - l/2)^2}} \right] \qquad (10)$$

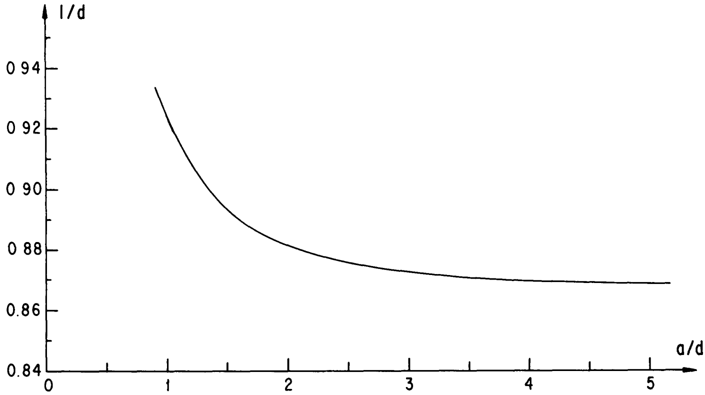

Fig. 3. Optimum length-to-diameter ratio l/d as a function of sensor-distance-to-diameter ratio a/d

where I_z is the axial component of magnetization. The corresponding field of a dipole is

$$H_{z,D} = 2\pi \cdot I_z \cdot \frac{r^2 l}{a^3}. \tag{11}$$

The radial field is given by the integral (using cylindrical coordinates)

$$H_r = 2 r l I_r \int_0^{\pi} \frac{(a - r\cos\theta)\cdot\cos\theta\, d\theta}{(r^2 + a^2 - 2ra\cos\theta)\sqrt{(l/2)^2 + r^2 + a^2 - 2ra\cos\theta}} \tag{12}$$

where I_r is the radial component of the magnetization. For every ratio a/d – where d is the diameter of the specimen – an optimum ratio l/d can be found where $H_r = H_z$. In this case no apparent anisotropy is observed although the specimen dimensions are comparable to the sample-detector separation. The optimum value of l/d according to formulae (10) and (12) is plotted as a function of a/d in Figure 3. As can be recognized, the optimum l/d ratio decreases with increasing a/d ratio. The anisotropy produced by a deviation from the optimum l/d value, of course, depends on the distance to the sensor. For a 5% error in l/d which is equal to a 1.1 mm change in length for a specimen with a diameter of 25.4 mm, some resulting anisotropy errors are given in Table 1. The change in

Table 1. Percentage anisotropy $\Delta k/k$ arising from a 5% error in l/d as a function of a/d

a/d	1.5	3	5
$\frac{\Delta(l/d)}{l/d}$	5%	5%	5%
$\frac{\Delta k}{k}$	1.4%	0.3%	0.1%

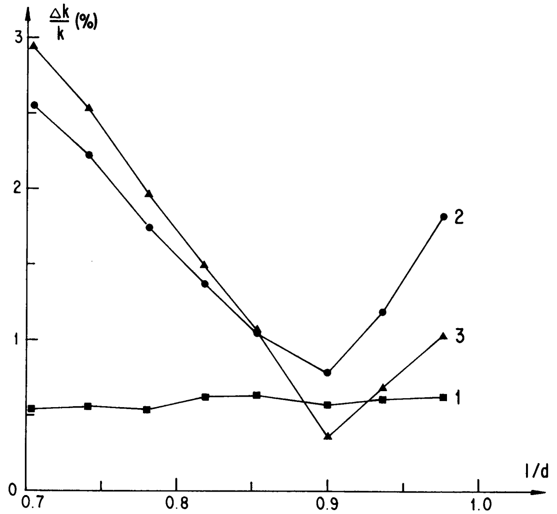

Fig. 4. Relative anisotropy values $\Delta k/k$ of a basalt specimen as a function of the length-to-diameter ratio l/d for the three planes of measurement: $\xi\eta$ (1), $\eta\zeta$ (2), $\zeta\xi$ (3). Instrument used: Digico anisotropy meter

anisotropy due to errors in l/d is of the correct order of magnitude to explain the observed anomalous behaviour of magnetic anisotropy in weakly anisotropic deep sea sediments which has been measured by means of a spinner magnetometer (Kent and Lowrie, 1975).

When the magnetic anisotropy of a specimen is measured using an inductive magnetometer the specimen size given by the ratio l/d has to be optimized, as the sensor distance is fixed by the given detector geometry. In order to find out the optimum size experimentally, we have sliced up some rock samples into sets of thin discs (each disc approximately 1 mm thick) which enabled us to measure the anisotropy as a function of l/d. It should be pointed out that the actual detecting coil geometries of both instruments are very complex or unknown to us in detail. Therefore it was not possible to measure or to calculate the effective a/d ratios.

Using the Digico anisotropy meter first, two tests have been carried out in order to determine the optimum l/d ratio for this instrument experimentally. Firstly, we have observed the change of percentage anisotropy $\Delta k/k$ as a function of l/d in each of the three measuring planes of a basalt sample which has a bulk susceptibility of $9.4 \cdot 10^{-4} G \cdot Oe^{-1}$. As basalts are very weakly anisotropic, $\Delta k/k$ should depend to a large extent on l/d when measuring in the $\zeta\xi$- or $\eta\zeta$-plane, respectively, and $\Delta k/k$ should be a minimum at the optimum l/d ratio. When measuring in the $\xi\eta$-plane $\Delta k/k$ should not be influenced by varying l/d ratios. The percentage anisotropy in each measuring plane is plotted in Figure 4. For the radial $\xi\eta$-plane $\Delta k/k$, as expected, does not change whereas a distinct minimum is found in the other two measuring planes for a ratio of $l/d = 0.9$. The anisotropy within the latter two planes decreases from about 3% at $l/d = 0.7$ to less than 1% at $l/d = 0.9$. It increases again above $l/d = 0.9$ with increasing l/d.

There is another possibility of determining the optimum l/d ratio. Not only

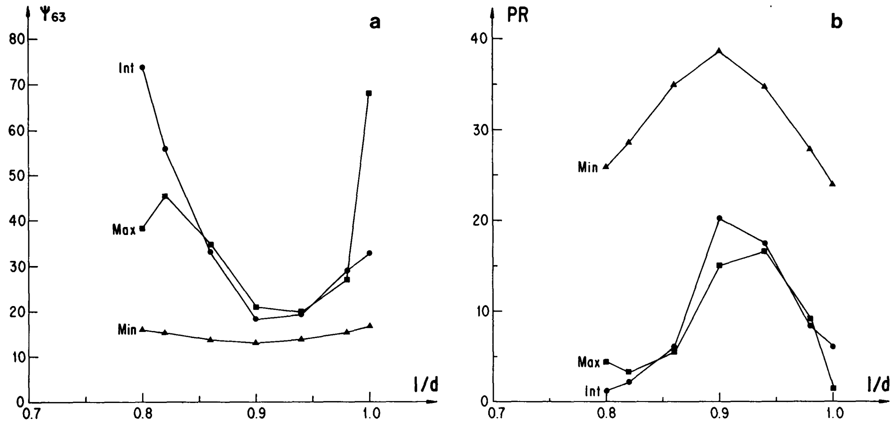

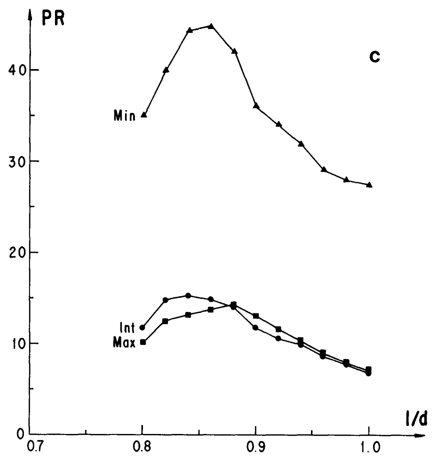

Fig. 5. a Angular standard deviation ψ_{63} and **b** precision parameter PR of the mean directions of principal anisotropy axes calculated for three tonalite specimens as a function of the length-to-diameter ratio l/d. Instrument used: Digico anisotropy meter. **c** Precision parameter PR as a function of l/d for the same specimens but measured with the ScT cryogenic magnetometer. Principal anisotropy axes: Max, Int, Min

the intensities but also the directions of the principal anisotropy axes depend on l/d. The dispersion of corresponding axes of different samples must pass through a minimum for the optimum l/d ratio. Two conditions have to be fulfilled for the validity of this test. Firstly the samples must have a macroscopic structure which is consistent throughout the region of investigation, and secondly they have to be oriented with respect to the macroscopic structure in different directions. Three tonalite specimens from Val Nambrone (Adamello massif, Northern Italy) having a mean bulk susceptibility of $2.7 \cdot 10^{-5}\, G \cdot \mathrm{Oe}^{-1}$ showed adequate properties in the above sense. The dispersion of their principal susceptibility axes expressed by the angular standard deviation ψ_{63} indicates a minimum for a l/d ratio of 0.90 ± 0.02 (Fig. 5a). The effect is especially pronounced for the maximum and intermediate axes, whereas the dispersion of the minimum axes is less affected. This is due to the fact that these rocks show a clearly visible schistosity which magnetically is reflected by a predominant oblate anisotropy ellipsoid. The computed precision parameter (Fisher, 1953) shows a corresponding maximum for the three principal axes for a value of $l/d = 0.90 \pm 0.02$ (Fig. 5b).

The dispersion test was applied to the cryogenic magnetometer, too (Fig. 5c). The precision parameter shows a less well defined but nevertheless distinct maximum for all three principal anisotropy axes at a ratio of $l/d=0.86\pm0.02$. The same quality of results was obtained before and after AF cleaning, although the remanence intensity observed before cleaning exceeded the differences of the induced magnetization ($H=1.01$ Oe) by one to two orders of magnitude.

We conclude from our measurements that the optimum values of l/d for the two instruments are slightly different due to varying pickup coil geometries. For our Digico anisotropy meter the optimum specimen length ($d=25.4$ mm) has been found to be $l=22.9\pm0.5$ mm, whereas for the ScT cryogenic magnetometer (3-axis-instrument with 38 mm access) the optimum length is a bit shorter with $l=21.8\pm0.5$ mm.

4. Instrumental Performance

In order to demonstrate the performance of the cryogenic magnetometer for the measurement of magnetic susceptibility anisotropy, a small scale regional investigation has been carried out in the Val Nambrone (Eastern Adamello massif, Northern Italy). As shown in Figure 6, the mean directions of the principal axes of the site susceptibility ellipsoids are fairly consistent throughout the whole area of investigation. They are in good agreement with the available data on the macroscopic structure (Callegari and Dal Piaz, 1973). The geological map presented by these authors shows a SW-NE trending schistosity in the area

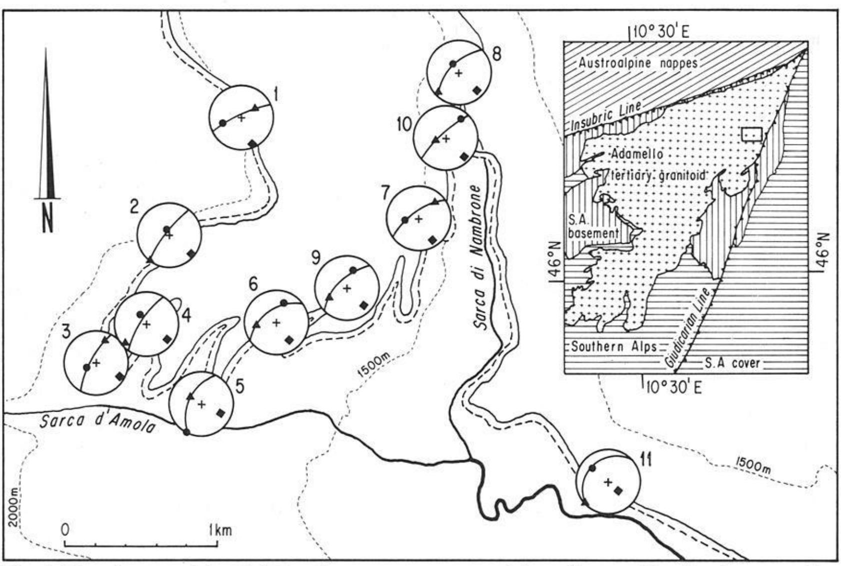

Fig. 6. Sketch map of the Val Nambrone area, eastern Adamello massif, with site mean directions of the principal anisotropy axes: maximum (●), intermediate (▲), minimum (◆). The great circle indicates the position of the main anisotropy plane

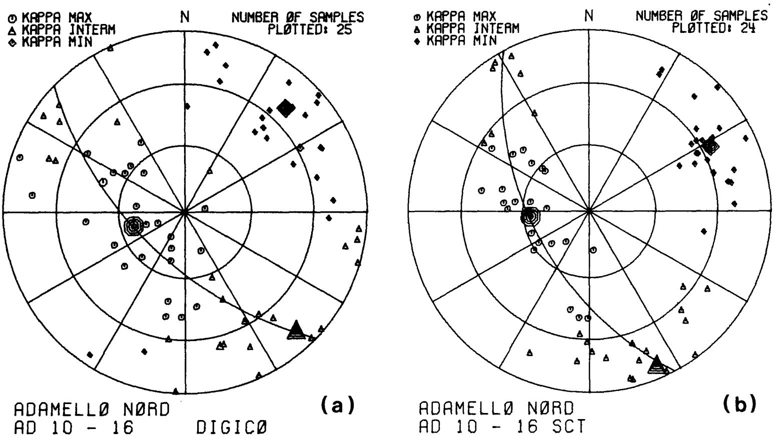

Fig. 7a and b. Lower hemisphere equal area projection of the directions of principal anisotropy axes for another sampling area in the northern Adamello massif (Italy) measured with the Digico anisotropy meter (**a**) and the ScT cryogenic magnetometer (**b**). The corresponding numerical mean values are listed in Table 2

Table 2. Mean directions of principal axes with precision parameter PR of a set of specimens from the northern Adamello massif as measured with the Digico and the ScT magnetometer. *N* denotes number of specimens

	k_{max}			k_{int}			k_{min}			
	Az.	Dip	PR	Az.	Dip	PR	Az.	Dip	PR	N
Digico	254.3	66.2	6.7	136.7	12.0	5.0	44.1	21.5	9.5	25
ScT	264.5	63.7	10.5	156.4	8.6	8.1	62.0	25.5	20.5	24

adjoining to the *E* of our sampling region. The very consistent alignment of the minimum axes of the sampling sites along a SE-NW direction – the minimum being perpendicular to the main anisotropy plane which obviously parallels the schistosity plane – indicates that the macroscopic structural features found at the eastern margin of the massif continue westward into the more central parts. The bulk susceptibility of the rocks has a well defined mean value of 2.66 $\pm 0.24 \cdot 10^{-5}\, G \cdot Oe^{-1}$ (number of specimens $N = 56$) which is in good agreement with the uniform tonalite petrology of the sampling area.

In order to compare results obtained from the cryogenic magnetometer and the Digico anisotropy meter, very weakly anisotropic samples have been measured on both instruments (cf. Fig. 7 and Table 2). Although the directions of the principal anisotropy axes are scattered to some extent, their mean directions coincide fairly well when comparing the results of both instruments. The mean directions and their precision parameters have been calculated independently for each axis. Both instruments show the best grouping of directions for the minimum axes, whereas the maximum and intermediate axes are distributed along a great circle.

Acknowledgements. We would like to thank Dr. J. Ansorge and Professor Dr. W. Lowrie for valuable discussions and critical reading of the manuscript. The suggestions of the unknown referees also are gratefully acknowledged.

References

Berset, G.: Eine Apparatur zur Messung kleiner remanenter Magnetisierungen an Gesteinen (Rockgenerator). Pageoph **69**, 205–228, 1968

Bhathal, R.S.: Magnetic anisotropy in rocks. Earth-Sci. Rev. **7**, 227–253, 1971

Callegari, E., Dal Piaz, G.: Field relationships between the main igneous masses of the Adamello intrusive massif (Northern Italy). Mem. Ist. Geol. Min. Univ. Padova **29**, 38, 1973

Fisher, R.A.: Dispersion on a sphere. Proc. Roy. Soc., London, Ser. A **217**, 295–305, 1953

Fuller, M.D.: Anisotropy of susceptibility and the natural remanent magnetisation of some Welsh slates. Nature **186**, 791–792, 1960

Goree, W.S., Fuller, M.: Magnetometers using RF-driven squids and their application in rock magnetism and paleomagnetism. Rev. Geophys. Space Phys. **14**, 591–608, 1976

Granar, L.: Magnetic measurements on Swedish varved sediments. Ark. Geofys. **3**, 1–40, 1958

Heller, F.: Magnetic anisotropy of granitic rocks of the Bergell massif (Switzerland). Earth Planet. Sci. Lett. **20**, 180–188, 1973

Ising, G.: On the magnetic properties of varved clay. Ark. Mat. Astr. Phys. **29** A, 1–37, 1943

Kent, D.V., Lowrie, W.: On the magnetic susceptibility anisotropy of deep-sea sediment. Earth Planet. Sci. Lett. **28**, 1–12, 1975

King, R.F., Rees, A.I.: Measurement of the anisotropy of magnetic susceptibility of rocks by the torque method. J. Geophys. Res. **67**, 1565–1572, 1962

Kubli, F.: Bau einer Apparatur zur Messung der magnetischen Suszeptibilität von Gesteinen. Diplomarbeit Inst. Geophysik ETH Zürich, unpublished, 1967

Noltimier, H.C.: Use of the spinner magnetometer for anisotropy measurements. In: Methods in palaeomagnetism, D.W. Collinson et al., eds.: pp. 399–402. Amsterdam: Elsevier 1967

Rees, A.I.: The effects of water currents in the magnetic remanence and anisotropy of susceptibility of some sediments. Geophys. J. Roy. Astron. Soc. **66**, 235–251, 1961

Rees, A.I.: The use of anisotropy of magnetic susceptibility in the estimation of sedimentary fabric. Sedimentology **4**, 257–271, 1965

Scriba, H.: Zusammenbau und Eichung einer Torsionswaage zur Messung der Anisotropie der Suszeptibilität von Gesteinen – Programmierung der Auswertung der Messungen. Diplomarbeit Inst. Geophysik ETH Zürich, unpublished, 1967

Sharma, P.V.: On the point dipole representation of a uniformly magnetised cylinder. Helv. Phys. Acta **38**, 234–240, 1965

Sharma, P.V.: Digital computation of gravitational and magnetic anomalies and their derivatives for two-dimensional bodies of arbitrary shape. Pageoph **64**, 14–18, 1966

Sharma, P.V.: Geophysical methods in geology, Amsterdam-Oxford-New York: Elsevier 1976

Sperner, E.: Einführung in die analytische Geometrie und Algebra, **2**, 4th ed. Göttingen: 1961

Stacey, F.D.: Magnetic anisotropy of igneous rocks. J. Geophys. Res. **65**, 2429–2442, 1960

Stone, D.B.: Torsion balance method of measuring anisotropic susceptibility, In: Methods in Palaeomagnetism, D.W. Collinson et al., eds.: pp. 381–386. Amsterdam: Elsevier 1967

Received December 12, 1977; Revised Version February 15, 1978